Int. J. Heat Mass Transfer. Vol. 27, No. 2, pp. 243–252, 1984
Printed in Great Britain

0017 9310/84 $3.00 + 0.00
Pergamon Press Ltd.

SHAPE OF POROUS REGION TO CONTROL COOLING ALONG CURVED EXIT BOUNDARY

ROBERT SIEGEL and AARON SNYDER
National Aeronautics and Space Administration, Lewis Research Center, Cleveland, OH 44135, U.S.A.

(*Received* 7 *October* 1982 *and in revised form* 25 *May* 1983)

Abstract—A cooled porous insert in a curved wall has a specified spatially varying heat flux applied to one side. It is desired to control the distribution of coolant flow out through this curved surface so that the surface will be kept at a desired uniform temperature. The flow regulation is accomplished by shaping the surface through which the coolant enters the region to obtain the required variation of flow resistance within the region. The proper surface shape is found by solving a Cauchy boundary value problem. Analytical solutions are given in two dimensions for various shapes of the heated boundary subjected to different heating distributions.

NOMENCLATURE

A shape parameter of curved heated surface
B amplitude of heated surface shape
c_p specific heat at constant pressure of coolant
D term defined after equation (35b)
E elliptic integral of the second kind
F elliptic integral of the first kind
H amplitude of heating variation along heated surface
$I_1 \ldots I_4$ functions defined after equation (35b)
k_m effective thermal conductivity of porous material
k modulus of elliptic integral, $k' = \sqrt{(1-k^2)}$
M for incompressible flow, $(1/2)(\mu/\mu_\infty)(t_\infty/t)$; for compressible flow, μ/μ_∞
n coordinate in direction of outward normal, Nw
P for incompressible flow, p/p_∞; for compressible flow, $(p/p_\infty)^2$
p pressure
q heat flow rate per unit area
$\mathbf{q}$ heat flux vector, equation (3)
R gas constant
$R_1 \ldots R_4$ functions defined after equation (35b)
s distance along curved boundary, Sw
T temperature ratio, t/t_∞
t absolute temperature
$\mathbf{u}$ coolant velocity vector
w width of porous region in the x-direction
X, Y Cartesian coordinates, x/w, y/w
X_0, Y_0 functions $X(\Psi)$, $Y(\Psi)$ along S_0
x, y Cartesian coordinates
Z complex variable, $X + iY$.

Greek symbols

α angle defined after equation (42b)
β angle defined after equation (42b)
ζ dummy integration variable
η variable, $\pi\Phi_s/\Psi_m$
θ angle in Fig. 3
κ permeability of porous material
λ parameter, $\rho_\infty c_p \kappa p_\infty / 2\mu_\infty k_m$
μ coolant viscosity
ξ variable, $\pi\Psi/\Psi_m$
ξ^* dummy variable
ρ coolant density
Φ potential function obtained by solving boundary value problem
Φ_s value of Φ obtained using equations (13) and (14)
φ amplitude of elliptic integral
χ quantity defined after equation (42b)
Ψ function orthogonal to Φ
Ψ_m maximum of Ψ
$\tilde{\nabla}^2$ $\partial^2/\partial X^2 + \partial^2/\partial Y^2$.

Subscripts

ref reference value
s at shaped coolant entrance surface
0 at curved boundary exposed to heat load (coolant exit surface)
∞ conditions in coolant reservoir.

INTRODUCTION

A POSSIBLE cooling technique for surface protection against high external heat fluxes is to use a porous structural material and force coolant through it so that it leaves the porous region through the heated boundary. Applications are in arc electrodes, turbine blades, rocket nozzles, and re-entry bodies. In the present analysis, the surface exposed to the heat load is curved and is required to be at uniform temperature even though the heat flux along it can be nonuniform. The required cooling can be achieved by utilizing the flow resistance within the porous region to obtain proper coolant distribution. The porous region surface at the coolant reservoir is shaped so that the necessary flow resistance is provided along paths through the region. The shape must be designed to yield the desired uniform temperature along the coolant exit surface. The analysis includes not only the effect of convective cooling within the porous region, but also the redistribution of energy by heat conduction in the porous metallic matrix.

The flow through the porous region is governed by Darcy's law, and can be compressible (perfect gas) or incompressible. Local thermal equilibrium is assumed between the coolant and the porous metallic matrix. The fluid viscosity can be a specified function of temperature. For these conditions a heat transfer theory has been developed and applied in refs. [1–4]. The heat transfer characteristics were shown to depend on obtaining a potential function in the region, so the mathematical problem is elliptic in type.

As discussed in ref. [4], the dual conditions of both temperature and heat flux being specified along the coolant exit boundary mean that the boundary conditions are of the Cauchy type. Consequently for an elliptic system the mathematical formulation is not well posed. Many useful solutions can be obtained, although it is not possible to find region shapes that will provide a desired performance for arbitrary heating conditions and surface shapes at the coolant exit boundary. A variety of solutions are given here for a class of cosine-like exit surface shapes. The heating conditions considered are uniform heat flux along the boundary, uniform unidirectional incident radiation, and a cosine type heating variation. The solutions illustrate the interactive effects on the inlet boundary of the exit boundary shape and the imposed heating conditions.

ANALYSIS

The two-dimensional (2-D) porous region is shown in Fig. 1. The curved upper and lower boundaries are permeable, while the side boundaries are joined to a solid wall and hence have no flow through them. The upper reservoir contains coolant at p_∞, t_∞ that is pumped into the region through boundary s. The coolant flows out through s_0 which is at uniform pressure p_0 and has a heat flux $q_0(x, y)$ imposed along it. The coolant flow distribution through s_0 is to be regulated to carry away this heat load and maintain the surface s_0 at a specified design temperature t_0. This is accomplished by having the proper shape of the upper curved surface. The correct region shape will provide the required flow distribution and heat conduction within the porous structure such that s_0 will be at the desired uniform temperature. In many instances the flow resistance of the porous medium is large enough that $p_\infty - p_0$ is much greater than any pressure variations along the porous boundaries. Hence p_∞ and p_0 can each be assumed uniform. The effect of nonuniform pressure can be estimated by using ref. [5].

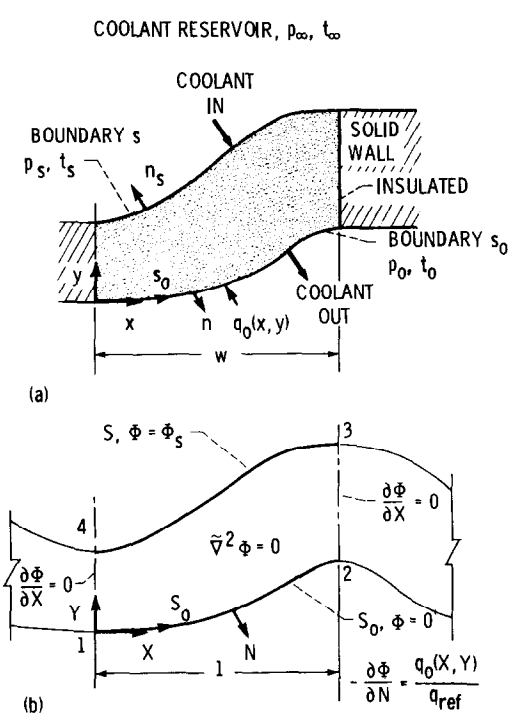

FIG. 1. Curved porous cooled insert in a solid wall: (a) physical coordinates and conditions at boundaries; (b) dimensionless coordinates with boundary conditions in terms of potential function.

General equations and boundary conditions

The differential equations of flow and energy have been developed and applied in refs. [1–4], and will now be briefly summarized. The relations allow for either compressible or incompressible flow, and for a coolant viscosity that is a function of temperature. The general equations are Darcy's law for flow through a porous material

$$\mathbf{u} = \frac{-\kappa}{\mu(t)} \nabla p, \tag{1}$$

(where κ is constant in the present analysis), conservation of mass

$$\nabla \cdot \mathbf{u} = 0 \text{ (incompressible flow)}, \tag{2a}$$

$$\nabla \cdot (\rho \mathbf{u}) = 0 \text{ (compressible flow)}. \tag{2b}$$

energy conservation for conditions of thermal equilibrium between solid and coolant

$$\nabla \cdot \mathbf{q} = 0 \quad \text{where} \quad \mathbf{q} = -k_m \nabla t + \rho \mathbf{u} c_p t, \tag{3}$$

and the perfect gas law for a compressible coolant

$$p = \rho R t. \tag{4}$$

The boundary conditions along the coolant inlet surface s are (upper surface in Fig. 1)

$$p = p_s = p_\infty = \text{const.}, \tag{5}$$

$$k_m \mathbf{n}_s \cdot \nabla t = \rho c_p (t - t_\infty) \mathbf{n}_s \cdot \mathbf{u}, \tag{6}$$

where $\mathbf{n}_s$ is a unit outward normal vector. Along the side boundaries, which are assumed insulated

$$\frac{\partial u}{\partial x} = 0, \tag{7a}$$

$$\frac{\partial t}{\partial x} = 0. \tag{7b}$$

Along the coolant exit surface s_0 of the region (the heated lower surface in Fig. 1)

$$p = p_0 = \text{const.}, \tag{8}$$

$$t = t_0 = \text{const.}, \tag{9}$$

$$k_m \left.\frac{\partial t}{\partial n}\right|_0 = q_0(x, y). \tag{10}$$

Potential function relations

Although the geometry is somewhat different, the analysis in ref. [4] involves boundary conditions similar to those of the present study. A key element shown by the analyses in refs. [1, 4] is that the spatial distributions of temperature, coolant flow, and heat flow within the porous region can all be expressed by analytical functions in terms of a potential function $\Phi(X, Y)$. The Φ is obtained by solving Laplace's

Physically, the negative gradient of Φ is proportional to the energy flux by both convection and conduction in the region [1].

After Φ has been found, the temperature distribution in the region is obtained by using

$$T(X, Y) = 1 + (T_0 - 1) \exp\left[-\frac{wq_{ref}}{k_m t_\infty (T_0 - 1)} \Phi(X, Y)\right]. \tag{11}$$

This particular form results from arbitrarily fixing the level of Φ such that at the lower boundary

$$\Phi(X, Y) = 0 \quad (X, Y \text{ on } S_0), \tag{12}$$

so that along S_0, $T(X, Y) = T_0$, which is the specified dimensionless surface temperature. At the upper boundary, equation (11) yields

$$\Phi_s = \frac{k_m t_\infty}{wq_{ref}} (T_0 - 1) \ln\left(\frac{T_0 - 1}{T_s - 1}\right), \tag{13}$$

where T_s and Φ_s are both uniform over S as shown by the derivations in refs. [1–3]. The upper boundary temperature T_s is not a specified quantity, but depends on the coolant flow rate and thus on the pumping pressure and coolant viscosity. The T_s is found from the relation [1–3]

$$P_0 = 1 + \frac{1}{\lambda} \int_{T_s}^{T_0} \frac{MT}{1 - T} \, dT, \tag{14}$$

where P_0 and T_0 are known, and the factor M accounts for the coolant viscosity variation with temperature inside the region. Along the side walls the boundary conditions in terms of Φ are

$$\frac{\partial \Phi}{\partial X} = 0. \tag{15}$$

By expressing t in terms of Φ by equation (11), the remaining boundary condition, equation (10), becomes

$$-\left.\frac{\partial \Phi}{\partial N}\right|_{\Phi = 0} = \frac{q_0(X, Y)}{q_{ref}}. \tag{16}$$

Figure 1(b) summarizes the conditions on Φ. The shape of the upper surface at constant Φ_s must be found to satisfy the dual boundary conditions (12) and (16) along the lower surface.

Region in potential plane, $W = \Psi + i\Phi$

The region in Fig. 1(b) extends between two constant Φ surfaces along 1–2 and 3–4, and the vertical sides are normal to the constant Φ lines. The region thus occupies a rectangle in the W-plane as shown in Fig. 2. The region can be extended in a periodic fashion in the X-direction by reflecting about the zero-derivative side boundaries (which become symmetry lines) as shown in Fig. 1(b); the transformed region then occupies an infinite strip in the upper half plane in Fig. 2. In what follows it will be necessary to describe Ψ (the function orthogonal to Φ) in terms of X, Y. When results are

In the W-plane the X, Y are dependent variables of Φ and Ψ. Since Φ and hence Ψ, are analytic functions of X, Y, then the X, Y are analytic functions of Ψ, Φ and satisfy

$$\frac{\partial^2 X}{\partial \Phi^2} + \frac{\partial^2 X}{\partial \Psi^2} = 0, \tag{17a}$$

$$\frac{\partial^2 Y}{\partial \Phi^2} + \frac{\partial^2 Y}{\partial \Psi^2} = 0, \tag{17b}$$

in the region bounded by $\Phi = 0$ and Φ_s. The Cauchy–Riemann equations then yield

$$\frac{\partial X}{\partial \Psi} = \frac{\partial Y}{\partial \Phi}, \tag{18a}$$

$$\frac{\partial X}{\partial \Phi} = -\frac{\partial Y}{\partial \Psi}. \tag{18b}$$

The Cauchy boundary conditions consist of specifying a function and its normal derivative along the same boundary. In terms of Fig. 2 this would consist of knowing $X(\Psi)$, $Y(\Psi)$, and $(\partial X/\partial \Phi)(\Psi)$, $(\partial Y/\partial \Phi)(\Psi)$ along the real axis 1–2 corresponding to the known boundary S_0 in Fig. 1. If these boundary conditions are known, the results in ref. [6; p. 689] can be used to derive an expression for $Z(\Psi, \Phi)$ in the region (as long as

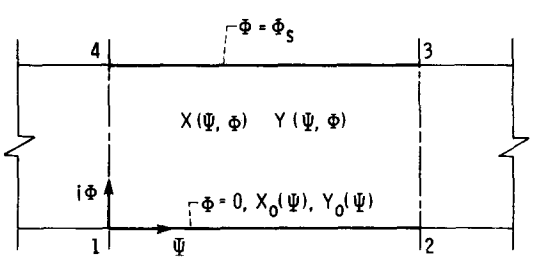

FIG. 2. Porous region in the potential plane $W = \Psi + i\Phi$.

Z remains analytic)

$$Z(\Psi,\Phi) = X(\Psi,\Phi)+iY(\Psi,\Phi) = \mathrm{Re}[X_0(\Psi+i\Phi)] + i\,\mathrm{Re}[Y_0(\Psi+i\Phi)] + \frac{1}{2i}\int_{\Psi-i\Phi}^{\Psi+i\Phi}\left[\left(\frac{\partial X}{\partial\Phi}\right)_0(\zeta) + i\left(\frac{\partial Y}{\partial\Phi}\right)_0(\zeta)\right]d\zeta. \quad (19)$$

Using the Cauchy–Riemann relations, equations (18a) and (18b), this is equal to

$$X(\Psi,\Phi)+iY(\Psi,\Phi) = \mathrm{Re}[X_0(\Psi+i\Phi)] + i\,\mathrm{Re}[Y_0(\Psi+i\Phi)] + \frac{1}{2i}\int_{\Psi-i\Phi}^{\Psi+i\Phi}\left[-\left(\frac{\partial Y}{\partial\Psi}\right)_0(\zeta) + i\left(\frac{\partial X}{\partial\Psi}\right)_0(\zeta)\right]d\zeta. \quad (20)$$

If the functions $X_0(\Psi)$ and $Y_0(\Psi)$ at the lower boundary are known, equation (20) can be integrated to yield Z in terms of known quantities

$$Z(\Psi,\Phi) = \mathrm{Re}[X_0(\Psi+i\Phi)]+i\,\mathrm{Re}[Y_0(\Psi+i\Phi)] + \frac{1}{2i}[-Y_0(\zeta)+iX_0(\zeta)]_{\Psi-i\Phi}^{\Psi+i\Phi}. \quad (21)$$

Since X_0 and Y_0 are real functions of a complex variable (i.e. the conjugate of the function equals the function of the conjugate), this simplifies to

$$Z(\Psi,\Phi) = X_0(\Psi+i\Phi)+iY_0(\Psi+i\Phi), \quad (22)$$

so that by separating real and imaginary parts

$$X(\Psi,\Phi) = \mathrm{Re}\ X_0(\Psi+i\Phi)-\mathrm{Im}\ Y_0(\Psi+i\Phi), \quad (23a)$$

$$Y(\Psi,\Phi) = \mathrm{Im}\ X_0(\Psi+i\Phi)+\mathrm{Re}\ Y_0(\Psi+i\Phi). \quad (23b)$$

As long as the solution is contained within a region in the upper half plane in which Z is analytic, the X, Y coordinates can be determined if the functions $X_0(\Psi)$ and $Y_0(\Psi)$ are known along $\Phi = 0$. These required X_0 and Y_0 relations can be found from the specified surface shape and imposed heat flux along the lower boundary in Fig. 1.

Since Φ and Ψ are analytic functions of X and Y we have the relations (referring to Fig. 3)

$$\left.\frac{\partial\Phi}{\partial N}\right|_0 \sin\theta = \left.\frac{\partial\Phi}{\partial X}\right|_0 = -\left.\frac{\partial\Psi}{\partial Y}\right|_0 = -\left.\frac{\partial\Psi}{\partial S}\right|_0 \sin\theta, \quad (24a)$$

$$\left.\frac{\partial\Phi}{\partial N}\right|_0 \cos\theta = -\left.\frac{\partial\Phi}{\partial Y}\right|_0 = -\left.\frac{\partial\Psi}{\partial X}\right|_0 = -\left.\frac{\partial\Psi}{\partial S}\right|_0 \cos\theta. \quad (24b)$$

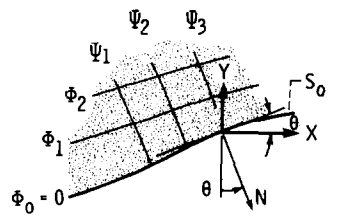

FIG. 3. Detail of normal direction along boundary S_0.

Hence, by using equation (16)

$$\left.\frac{\partial\Phi}{\partial N}\right|_0 = -\frac{q_0(X,Y)}{q_{\mathrm{ref}}} = -\left.\frac{\partial\Psi}{\partial S}\right|_0, \quad (25)$$

which is also a Cauchy–Riemann equation since N and S are orthogonal. Integrating for Ψ as a function of S_0 (let $\Psi = 0$ at $S_0 = 0$)

$$\Psi(X,Y) = \int_0^{S_0(X,Y)} \frac{q_0(X,Y)}{q_{\mathrm{ref}}}\,dS_0 \quad (X, Y \text{ on } S_0). \quad (26)$$

With $S_0(X, Y)$ and $q_0(X, Y)$ specified, equation (26) will provide the necessary relations for calculating X and Y from equations (23a) and (23b). When $\Phi = \Phi_s$, where the value of Φ_s is found from equation (13) in conjunction with equation (14) for the specified physical conditions, then equations (23a) and (23b) will yield the coordinates of the unknown upper surface in Fig. 1(b). Results will now be obtained for some specific heating conditions.

Results for various heating conditions

Heat radiation in the Y-direction that is uniform with X. As a first example, unidirectional radiative heating provides an especially simple analytical solution; the heating is shown in Fig. 4. If α is the absorptivity of the surface for radiation, the heat flux along S_0 is $q_0(S) = q_{\mathrm{rad}}\alpha\cos\theta(S)$. The surface temperature is assumed sufficiently low so that reradiation can be neglected. From equation (26), since $dS/dX|_0 = 1/\cos\theta$, there results along S_0 (let $q_{\mathrm{ref}} \equiv \alpha q_{\mathrm{rad}}$)

$$\Psi(X,Y) = \int_0^{X(S_0)} \cos\theta(S)\left.\frac{dS}{dX}\right|_0 dX = \int_0^{X_0} dX = X_0. \quad (27)$$

Then by use of equation (27) in equations (23a) and (23b)

$$X(\Psi,\Phi) = \mathrm{Re}\ (\Psi+i\Phi)-\mathrm{Im}\ Y_0(\Psi+i\Phi), \quad (28a)$$

$$Y(\Psi,\Phi) = \mathrm{Im}\ (\Psi+i\Phi)+\mathrm{Re}\ Y_0(\Psi+i\Phi), \quad (28b)$$

where $Y_0(\Psi) = Y_0(X)$ by virtue of equation (27), and $Y_0(X)$ is the specified shape of the heated lower boundary in Fig. 4. This type of solution is related to the results for an inverse electrochemical machining problem analyzed in ref. [7].

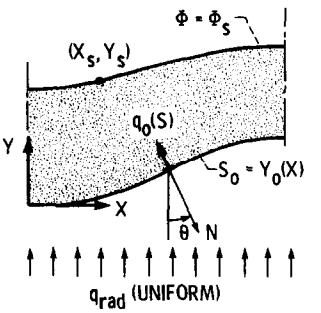

FIG. 4. Heating by uniform radiation directed parallel to Y-axis.

A convenient periodic function that will define a variety of shapes for the lower boundary, by using various A and B, is

$$Y_0(X) = \frac{B(1-A)}{2A}\left(\frac{1+A}{1+A\cos\pi X} - 1\right) \quad -1 < A < 1. \tag{29}$$

The $Y_0(0) = 0$ and $Y_0(1) = B$ (the amplitude of the curve), and A regulates the shape as shown by the sets of curves for $\Phi_s = 0$ (labeled 'lower boundary') in Figs. 5(a) and (b). Using equation (29) [and $Y_0(X) = Y_0(\Psi)$ from equation (27)] in equations (28a) and (28b) yields for the coordinates of the upper surface ($0 \leqslant \Psi \leqslant 1$, $\Phi = \Phi_s > 0$)

$$X_s = \Psi - \frac{B(1-A^2)}{2}\left[\frac{\sin\pi\Psi\sinh\pi\Phi_s}{(1+A\cos\pi\Psi\cosh\pi\Phi_s)^2+(A\sin\pi\Psi\sinh\pi\Phi_s)^2}\right], \tag{30a}$$

$$Y_s = \Phi_s + \frac{B(1-A)}{2A}\left[\frac{(1+A)(1+A\cos\pi\Psi\cosh\pi\Phi_s)}{(1+A\cos\pi\Psi\cosh\pi\Phi_s)^2+(A\sin\pi\Psi\sinh\pi\Phi_s)^2} - 1\right]. \tag{30b}$$

When the shape parameter $A = 0$, the lower boundary is a simple cosine curve and the coordinates of the upper surface become

$$X_s = \Psi - \left(\frac{B}{2}\right)\sin\pi\Psi\sinh\pi\Phi_s,$$

$$Y_s = \Phi_s + \left(\frac{B}{2}\right)(1-\cos\pi\Psi\cosh\pi\Phi_s).$$

Results for upper surface shapes ($\Phi_s > 0$) are given in Fig. 5 and will be discussed later.

Uniform heat flux along S_0 for a class of small amplitude cosine-like surfaces. If a uniform heat flux is applied along the lower surface, then $q_0(X, Y)/q_{ref} = 1$ and from equation (26), $\Psi = S_0$. Then $(\partial S/\partial\Psi)_0^2 = 1 = (\partial X/\partial\Psi)_0^2 + (\partial Y/\partial\Psi)_0^2$ and $X_0(\Psi)$ along the lower surface can be found from

$$X_0(\Psi) = \int_0^{\Psi}\left[1-\left(\frac{\partial Y}{\partial\Psi}\right)_0^2\right]^{1/2} d\Psi. \tag{31}$$

The maximum value of $\Psi \equiv \Psi_m$ is found by integrating over the entire S_0 which extends to $X_0 = 1$

$$1 = \int_0^{\Psi_m}\left[1-\left(\frac{\partial Y}{\partial\Psi}\right)_0^2\right]^{1/2} d\Psi. \tag{32}$$

The effect of the lower surface shape can be conveniently studied by letting

$$Y_0(\Psi) = \frac{B(1-A)}{2A}\left[\frac{1+A}{1+A\cos(\pi\Psi/\Psi_m)} - 1\right], \tag{33}$$

and also letting the amplitude B be small enough so that $B^2 \ll 1$ (note that at the end of the curve where $X_0 = 1$ and $\Psi = \Psi_m$, the $Y_0 = B$). This form is chosen because for small B, the Ψ/Ψ_m is close to X in value as found from equation (31); hence the shapes of S_0 are close to those in equation (29) and comparisons can be made. Equation (33) is substituted into equation (31) and the square root expanded for small B to obtain

$$X_0(\Psi) = \int_0^{\Psi}\left\{1 - \frac{1}{2}\left[\frac{B\pi}{2\Psi_m}(1-A^2)\right]^2 \times \frac{\sin^2(\pi\Psi/\Psi_m)}{[1+A\cos(\pi\Psi/\Psi_m)]^4}\right\} d\Psi. \tag{34}$$

The integration is carried out and the result, along with equation (33), is substituted into equations (23a) and

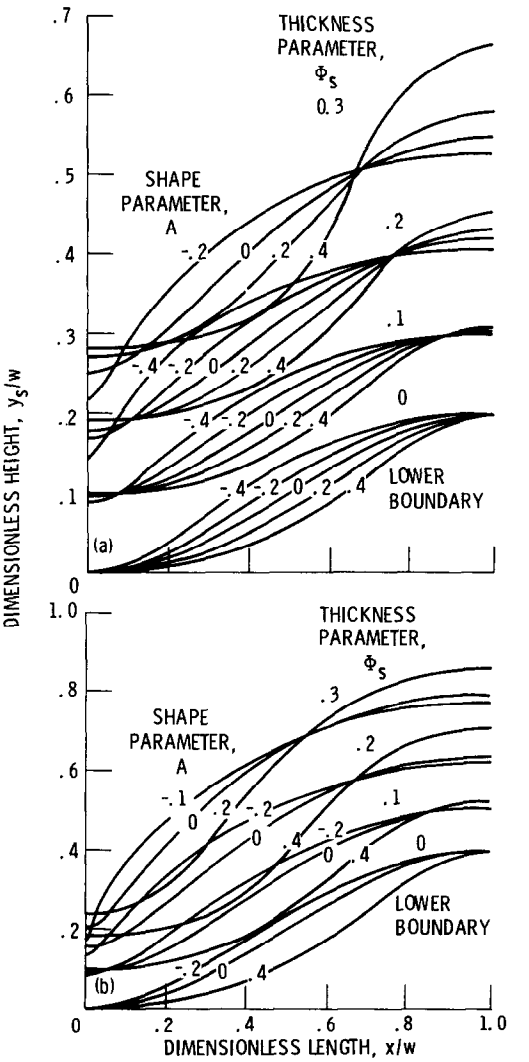

FIG. 5. Shape of porous region for heating of lower boundary by uniform radiation directed parallel to y-axis: (a) amplitude of lower boundary $B = 0.2$; (b) amplitude of lower boundary $B = 0.4$.

(23b). After considerable algebra, this yields

$$X_s = \Psi + \frac{\Psi_m}{2\pi}\left[\frac{B\pi}{2\Psi_m}(1-A^2)\right]^2\left\{\frac{1+2A^2}{6A(1-A^2)^2}\frac{R_1}{D} + \frac{1}{6A(1-A^2)}\frac{R_2}{D^2} - \frac{1}{3A}\frac{R_3}{D^3} - \frac{1}{(1-A^2)^{5/2}}\frac{1}{2}\tan^{-1}\frac{2R_4}{1-R_4^2-I_4^2}\right\} - \frac{B(1-A)}{2}\frac{(1+A)\sin\xi\sinh\eta}{D(\xi,\eta)}. \quad (35a)$$

(Note that the quadrant for $\tan^{-1}$ is according to the individual signs of the numerator and denominator.)

$$Y_s = \Phi_s + \frac{\Psi_m}{2\pi}\left[\frac{B\pi}{2\Psi_m}(1-A^2)\right]^2\left\{\frac{1+2A^2}{6A(1-A^2)^2}\frac{I_1}{D} + \frac{1}{6A(1-A^2)}\frac{I_2}{D^2} - \frac{1}{3A}\frac{I_3}{D^3} - \frac{1}{(1-A^2)^{5/2}}\frac{1}{4}\ln\frac{(1+I_4)^2+R_4^2}{(1-I_4)^2+R_4^2}\right\} + \frac{B(1-A)}{2A}\left[\frac{(1+A)(1+A\cos\xi\cosh\eta)}{D(\xi,\eta)} - 1\right], \quad (35b)$$

where $\xi = \pi\Psi/\Psi_m$, $\eta = \pi\Phi_s/\Psi_m$, Ψ_m is found from

$$\Psi_m = \frac{1}{2} + \frac{1}{4}\left[4 + \frac{(B\pi)^2}{\sqrt{(1-A^2)}}\right]^{1/2},$$

$$D(\xi,\eta) = (1+A\cos\xi\cosh\eta)^2 + (A\sin\xi\sinh\eta)^2,$$

$$R_1 = \sin\xi(\cosh\eta + A\cos\xi),$$

$$I_1 = \sinh\eta(\cos\xi + A\cosh\eta),$$

$$R_2 = \sin\xi[\cosh\eta + 2A\cos\xi + A^2\cosh\eta(\cos^2\xi - \sinh^2\eta)],$$

$$I_2 = \sinh\eta[\cos\xi + 2A\cosh\eta + A^2\cos\xi(\sin^2\xi + \cosh^2\eta)],$$

$$R_3 = \sin\xi[\cosh\eta + 3A\cos\xi + 3A^2\cosh\eta(\cos^2\xi - \sinh^2\eta) + A^3\cos\xi(\cosh^2\eta\cos^2\xi - 2\cosh^2\eta\sinh^2\eta - \sin^2\xi\sinh^2\eta)],$$

$$I_3 = \sinh\eta[\cos\xi + 3A\cosh\eta + 3A^2\cos\xi(\cosh^2\eta + \sin^2\xi) + A^2\cosh\eta(\cosh^2\eta\cos^2\xi + 2\cos^2\xi\sin^2\xi - \sin^2\xi\sinh^2\eta)],$$

$$R_4 = \sqrt{\left(\frac{1-A}{1+A}\right)}\frac{\sin\xi}{\cos\xi + \cosh\eta},$$

$$I_4 = \sqrt{\left(\frac{1-A}{1+A}\right)}\frac{\sinh\eta}{\cos\xi + \cosh\eta}.$$

Results are given in Fig. 6 where the upper surface shapes are for $\Phi_s > 0$.

Nonuniform heating along a cosine-like lower surface (small amplitudes). The purpose of this example is to illustrate in a relatively simple way how the shape of the upper surface is influenced by the combined effects of having the lower surface curved and also having the heating along it be nonuniform. Let

$$Y_0(\Psi) = \frac{B}{2}\left(1 - \cos\pi\frac{\Psi}{\Psi_m}\right), \quad (36)$$

and

$$\frac{q_0(\Psi)}{q_{ref}} = 1 + \frac{H}{2}\left(1 - \cos\pi\frac{\Psi}{\Psi_m}\right). \quad (37)$$

Then using $(\partial S/\partial\Psi)_0^2 = 1/(q_0/q_{ref})^2 = (\partial X/\partial\Psi)_0^2 + (\partial Y/\partial\Psi)_0^2$ gives

$$\left.\frac{\partial X}{\partial\Psi}\right|_0 = \left\{\frac{1}{\left[1 + \frac{H}{2}\left(1 - \cos\pi\frac{\Psi}{\Psi_m}\right)\right]^2 - \left(\frac{B}{2}\frac{\pi}{\Psi_m}\right)^2\sin^2\left(\pi\frac{\Psi}{\Psi_m}\right)}\right\}^{1/2}.$$

The results will now be limited to both amplitudes B and H being small so that by expanding in powers of B and H, and neglecting powers higher than the square, the $X_0(\Psi)$ becomes

$$X_0(\Psi) = \int_0^\Psi\left[1 - \frac{H}{2}\left(1 - \cos\pi\frac{\Psi}{\Psi_m}\right) + \frac{H^2}{4}\left(1 - \cos\pi\frac{\Psi}{\Psi_m}\right)^2 - \frac{1}{2}\left(\frac{B}{2}\frac{\pi}{\Psi_m}\right)^2\sin^2\pi\frac{\Psi}{\Psi_m}\right]d\Psi.$$

Carrying out the integration yields

$$X_0(\Psi) = \frac{\Psi_m}{\pi}\left\{\left[1 - \frac{H}{2} + \frac{3H^2}{8} - \left(\frac{B}{4}\frac{\pi}{\Psi_m}\right)^2\right]\times\pi\frac{\Psi}{\Psi_m} + \frac{H}{2}(1-H)\sin\pi\frac{\Psi}{\Psi_m} + \left[\left(\frac{H}{4}\right)^2 + \frac{1}{2}\left(\frac{B}{4}\frac{\pi}{\Psi_m}\right)^2\right]\sin 2\pi\frac{\Psi}{\Psi_m}\right\}. \quad (38)$$

The Ψ_m is found by using $\Psi = \Psi_m$ at $X_0 = 1$ which yields

$$\Psi_m = \frac{1 + \left[1 + 4\left(1 - \frac{H}{2} + \frac{3H^2}{8}\right)\left(\frac{B\pi}{4}\right)^2\right]^{1/2}}{2\left(1 - \frac{H}{2} + \frac{3H^2}{8}\right)}.$$

When equations (37) and (38) are substituted into equation (23a) and (23b), the results for the coordinates

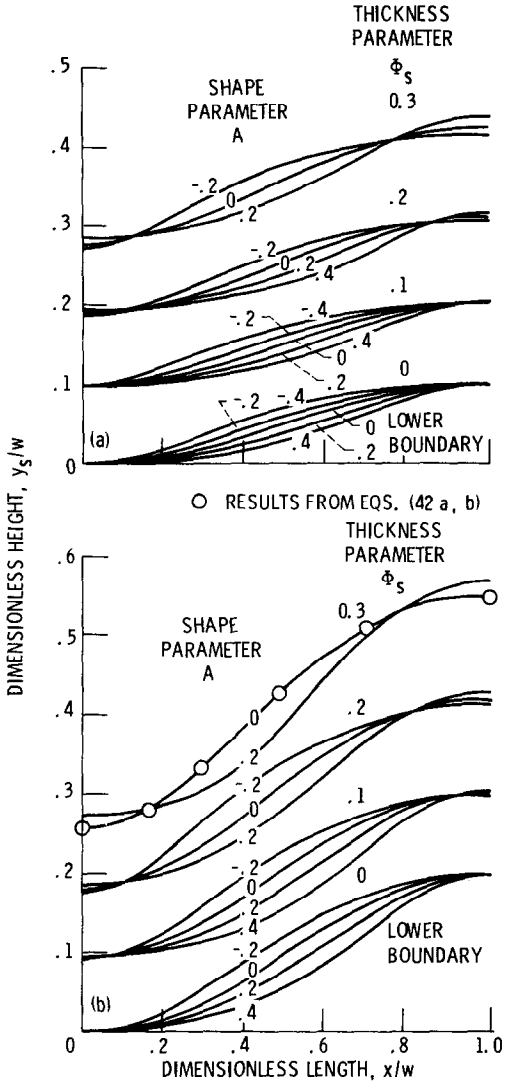

FIG. 6. Shape of porous region for uniform heat flux along lower surface: (a) amplitude of lower boundary $B = 0.1$; (b) amplitude of lower boundary $B = 0.2$.

of the unknown upper surface are

$$X_s = \frac{\Psi_m}{\pi}\left\{\left[1-\frac{H}{2}+\frac{3H^2}{8}-\left(\frac{B}{4}\frac{\pi}{\Psi_m}\right)^2\right]\xi + \frac{H}{2}(1-H)\sin\xi\cosh\eta+\left[\left(\frac{H}{4}\right)^2+\frac{1}{2}\left(\frac{B}{4}\frac{\pi}{\Psi_m}\right)^2\right] \times\sin 2\xi\cosh 2\eta\right\}-\frac{B}{2}\sin\xi\sinh\eta, \quad (39a)$$

$$Y_s = \frac{\Psi_m}{\pi}\left\{\left[1-\frac{H}{2}+\frac{3H^2}{8}-\left(\frac{B}{4}\frac{\pi}{\Psi_m}\right)^2\right]\eta + \frac{H}{2}(1-H)\cos\xi\sinh\eta+\left[\left(\frac{H}{4}\right)^2+\frac{1}{2}\left(\frac{B}{4}\frac{\pi}{\Psi_m}\right)^2\right] \times\cos 2\xi\sinh 2\eta\right\}+\frac{B}{2}(1-\cos\xi\cosh\eta). \quad (39b)$$

Shapes are given in Fig. 7 for the lower boundaries ($\Phi_s = 0$) and the corresponding upper boundaries ($\Phi_s > 0$).

Uniform heat flux along a cosine-like surface (not restricted to small amplitude). The results that follow can be used to examine the effect of larger amplitudes of the lower surface curvature, and will verify the small amplitude approximation used for calculating Fig. 6. If a cosine relation for Y_0 in terms of Ψ

$$Y_0(\Psi) = \frac{B}{2}\left(1-\cos\pi\frac{\Psi}{\Psi_m}\right), \quad (40)$$

is inserted into equation (31) for uniform boundary heat flux, the result is

$$X_0(\Psi) = \int_0^{\Psi}\left[1-\left(\frac{B}{2}\frac{\pi}{\Psi_m}\right)^2\sin^2\pi\frac{\Psi}{\Psi_m}\right]^{1/2}d\Psi.$$

This is an elliptic integral of the second kind

$$E(\varphi,k)\equiv\int_0^{\varphi}[1-k^2\sin^2\zeta]^{1/2}\,d\zeta,$$

and can be written in the form (using $k = \pi B/2\Psi_m$)

$$X_0(\Psi) = \frac{\Psi_m}{\pi}E\left(\pi\frac{\Psi}{\Psi_m},k\right)\quad 0\leqslant\frac{\Psi}{\Psi_m}\leqslant\frac{1}{2}, \quad (41a)$$

$$X_0(\Psi) = 1-\frac{\Psi_m}{\pi}E\left(\pi\frac{\Psi_m-\Psi}{\Psi_m},k\right)\quad \frac{1}{2}\leqslant\frac{\Psi}{\Psi_m}\leqslant 1. \quad (41b)$$

Using the condition that $X_0(\Psi_m) = 1$ yields an implicit relation for determining Ψ_m from the amplitude B of the lower surface

$$1 = \left(\frac{2\Psi_m}{\pi}\right)E\left(\frac{\pi}{2},k\right).$$

Equations (40) and (41) are substituted into equations (23a) and (23b) to yield

$$\left.\begin{aligned} X_s &= \frac{\Psi_m}{\pi}\,\mathrm{Re}\,E\left[\frac{\pi}{\Psi_m}(\Psi+i\Phi_s),k\right]-\frac{B}{2}\sin\pi\frac{\Psi}{\Psi_m}\sinh\pi\frac{\Phi_s}{\Psi_m}\\ Y_s &= \frac{\Psi_m}{\pi}\,\mathrm{Im}\,E\left[\frac{\pi}{\Psi_m}(\Psi+i\Phi_s),k\right]+\frac{B}{2}\left(1-\cos\pi\frac{\Psi}{\Psi_m}\cosh\pi\frac{\Phi_s}{\Psi_m}\right)\end{aligned}\right\}\quad 0\leqslant\frac{\Psi}{\Psi_m}\leqslant\frac{1}{2}, \quad (42a)$$

$$\left.\begin{aligned} X_s &= 1-\frac{\Psi_m}{\pi}\,\mathrm{Re}\,E\left[\frac{\pi}{\Psi_m}(\Psi_m-\Psi-i\Phi_s),k\right]-\frac{B}{2}\sin\pi\frac{\Psi}{\Psi_m}\sinh\pi\frac{\Phi_s}{\Psi_m}\\ Y_s &= -\frac{\Psi_m}{\pi}\,\mathrm{Im}\,E\left[\frac{\pi}{\Psi_m}(\Psi_m-\Psi-i\Phi_s),k\right]+\frac{B}{2}\left(1-\cos\pi\frac{\Psi}{\Psi_m}\cosh\pi\frac{\Phi_s}{\Psi_m}\right)\end{aligned}\right\}\quad \frac{1}{2}\leqslant\frac{\Psi}{\Psi_m}\leqslant 1. \quad (42b)$$

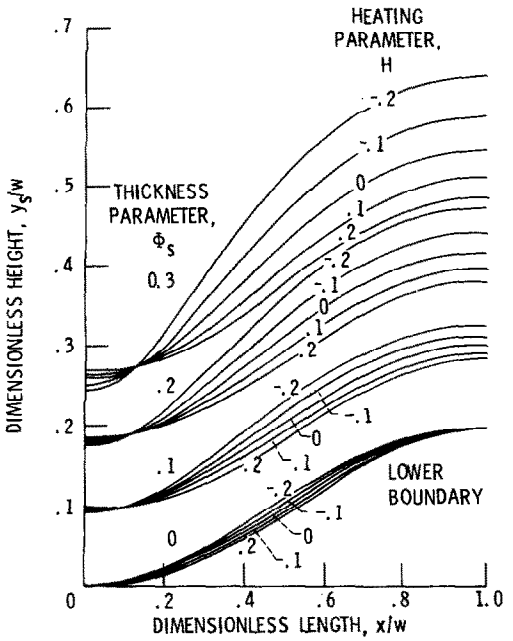

FIG. 7. Porous region shapes for nonuniform heating along an almost cosine shaped lower boundary.

The real and imaginary parts of E are found from the following [8]:

$$\text{Re } E(\xi^* \pm i\eta, k) = E(\beta, k) + \frac{k^2 \sin\beta \cos\beta \sin^2\alpha \sqrt{(1-k^2\sin^2\beta)}}{\cos^2\alpha + k^2 \sin^2\beta \sin^2\alpha},$$

$$\text{Im } E(\xi^* \pm i\eta, k) = \pm\left[F(\alpha, k') - E(\alpha, k') + \frac{(1-k^2\sin^2\beta)\sin\alpha\cos\alpha\sqrt{(1-k'^2\sin^2\alpha)}}{\cos^2\alpha + k^2\sin^2\beta\sin^2\alpha}\right],$$

where

$$k' = \sqrt{(1-k^2)}$$

and

$$F(\varphi, k) \equiv \int_0^{\varphi} \frac{d\zeta}{\sqrt{(1-k^2\sin^2\zeta)}}$$

(the elliptic integral of the first kind). The β is found from $\beta = \cot^{-1}\sqrt{\chi}$ where χ is the positive root of the quadratic equation

$$\chi^2 - (\cot^2\xi^* + k^2\sinh^2\eta\,\text{cosec}^2\,\xi^* - k'^2)\chi - k'^2\cot^2\xi^* = 0.$$

The α is found from

$$\alpha = \tan^{-1}\left[\frac{1}{k}(\tan^2\xi^*\cot^2\beta - 1)^{1/2}\right].$$

At the end points $\Psi = 0$ and $\Psi = \Psi_m$, the $\xi^* = 0$ and the value of $E(\pm i\eta, k)$ is imaginary. In this instance a special formula in ref. [8; p. 592] is used to obtain

$$X(0, \Phi_s) = 0,$$

$$Y(0, \Phi_s) = \frac{\Psi_m}{\pi}[-E(\theta, K) + F(\theta, K) + \sqrt{(1-\cos^2\alpha\sin^2\theta)}\tan\theta] + \frac{B}{2}\left(1 - \cosh\frac{\pi\Phi_s}{\Psi_m}\right),$$

where

$$\theta = \tan^{-1}\left(\sinh\frac{\pi\Phi_s}{\Psi_m}\right),$$

$$\alpha = \sin^{-1}k, K = \sin\left(\frac{\pi}{2} - \alpha\right),$$

$$X(\Psi_m, \Phi_s) = 1,$$

$$Y(\Psi_m, \Phi_s) = Y(0, \Phi_s) + B\cosh\frac{\pi\Phi_s}{\Psi_m}.$$

At the specific location where $\Psi/\Psi_m = 0.5$, $\chi = 0$ and $\beta = \pi/2$. The α is found from the limiting expression

$$\alpha = \tan^{-1}\left[\frac{1}{k}\left(\frac{k'^2}{k'^2 - k^2\sinh^2\eta} - 1\right)^{1/2}\right].$$

Results for upper and lower boundary shapes are given in Fig. 8.

RESULTS AND DISCUSSION

When the lower surface s_0 of the porous material, through which the coolant exists, is heated by incident radiation in the y-direction that is uniform with x as shown in Fig. 4, the coordinates of the upper surface s are given by equations (30a) and (30b). These shapes of

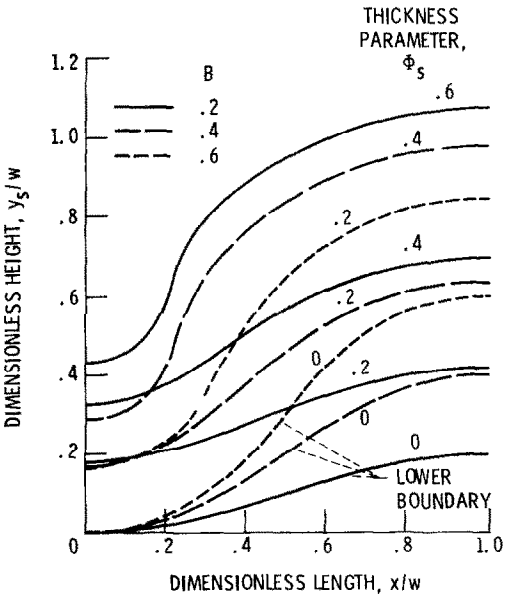

FIG. 8. Porous region shapes for uniform heat flux along cosine-like lower boundaries of large amplitude.

s will yield uniform temperature along s_0 as achieved by regulating both the energy convection in the porous region and the redistribution of energy by heat conduction in the metallic matrix. Lower boundary shapes corresponding to equations (30a) and (30b) are given by equation (29). The amplitude of the curve is B, and the parameter A provides a shape variation; for $A = 0$ the s_0 is a cosine curve. For various A values and for $B = 0.2$ and 0.4, the porous region shapes are shown in Fig. 5 where the lower boundary curves correspond to $\Phi_s = 0$ and the upper boundaries are for $\Phi_s > 0$. The Φ_s is the value of the potential function at the upper surface where the coolant enters the porous region. The Φ_s is found from the imposed pressures and temperatures by equations (13) and (14), and determines the average thickness of the region; the thickness increases as Φ_s is increased (the thickness is zero when $\Phi_s = 0$). As shown by equation (13) an increase in heating rate (increased q_{ref}) yields a decreased Φ_s and hence decreased region thickness; this provides the required increased coolant flow.

Figure 5 shows only some examples of the upper boundary shapes since results for other parameters are easily calculated from the analytical solution. For thin regions and a small amplitude B the upper contour tends to follow the lower contour. This is because, for small curvature (small B), radiative heating provides practically uniform heat addition along the lower surface. For a thin region the behavior tends to be locally one-dimensional (1-D); the result is a region of practically uniform thickness.

As Φ_s, and hence the thickness, becomes larger the upper contour deviates increasingly from being locally 1-D. For small x the lower contour is convex and hence the flow from the upper boundary is somewhat like flow through a cylindrical wall from inside to outside. At large x the lower surface is concave and the flow is like inward flow in a cylindrical region. The fact that the region tends to be thin at small x and thick at large x reflects the difference in flow resistance for these two geometrical configurations. For larger thicknesses it becomes more difficult to control the flow at the exit surface by means of shaping the upper surface. It is physically evident that if the lower boundary were very irregular it would not be possible to find an upper surface shape that would properly control the exit coolant distribution. This is the nature of a Cauchy problem for an elliptic system; it is not possible to obtain a solution for arbitrary boundary conditions. In the calculations this will be revealed by the appearance of negative X_s and/or Y_s, or a shape that is obviously unreasonable. As $|A|$, B, Φ_s, or any combination of values is increased there is a greater possibility that the solution will not exist. By avoiding regions that are thick it is possible to obtain solutions of practical use.

For uniform heating along the lower boundary, Fig. 6 provides results calculated from equations (35a) and (35b). The approximation used in the derivation limits these particular results to small B, so results are given for $B = 0.1$ and 0.2. The validity of the approximation is shown in Fig. 6(b) where the circular symbols on the curve for $A = 0$ and $\Phi_s = 0.3$ are from the solution not limited to small B, equations (42a) and (42b). The results in Fig. 6 have the same general behavior as those in Fig. 5 for unidirectional radiative heating. It was found somewhat more difficult to meet the requirement of uniform heating, so there are not as many A values in Fig. 6(b) compared with Fig. 5(a) (which is also for $B = 0.2$).

For nonuniform heating along the curved lower boundary some results are shown in Fig. 7. Increased heating requires a smaller region thickness to provide a greater coolant flow. From equation (37) a positive value of the heating parameter H corresponds to increased heating along the x-direction (note that for small H and B the Ψ is not too different from X). Hence when $H = 0.2$ for example, the thinning effect required by increased heating with x counteracts the geometric effect of the lower surface becoming concave as x/w approaches 1. The result is a layer of practically uniform thickness in the y-direction. When the heating decreases with x (negative H) the nonuniform heating and geometric effects combine to cause the layer thickness to increase significantly with x.

The theory leading to equations (42a) and (42b) is not limited to small B values for the heated surface. Results are given in Fig. 8 for $B = 0.2$, 0.4, and 0.6, that demonstrate the more extreme shaping required for the upper surface as B is increased. A larger B limits the possible solutions to smaller Φ_s values. Some values from equations (42a) and (42b) are also included on one curve in Fig. 6(b) where the good agreement demonstrates the validity of the small B approximation.

CONCLUDING REMARKS

An analytical method has been devised for determining the shape of a cooled porous insert in a curved wall to meet certain boundary conditions. One curved side of the insert is subjected to nonuniform heating and is to be maintained at a uniform temperature according to design constraints. Coolant is forced through the porous region from a reservoir on the other side of the insert, and leaves through the heated boundary. The heat transfer in the porous matrix is controlled by both convection and conduction. The shape of the boundary at the reservoir side is unknown and is to be determined so that the region shape will properly regulate the coolant to achieve the required boundary conditions. Since both heat flux and temperature are specified along one boundary the problem is of the Cauchy boundary value type. The mathematical nature of an elliptic system of this type limits the generality of the solutions that can be obtained. Solutions are most easily obtained for thin regions, and when the contour of the heated surface and the heating along it are not too irregular. A variety of results are obtained to show how the porous region should be designed to meet a required heat transfer performance.

REFERENCES

1. R. Siegel and M. E. Goldstein, Analytical solution for heat transfer in three-dimensional porous media including variable fluid properties, TN D-6941, NASA, September (1972).
2. R. Siegel, Shape of porous cooled region for surface heat flux and temperature both specified, *Int. J. Heat Mass Transfer* **16,** 1807–1811 (1973).
3. R. Siegel, Analysis of shape of porous cooled medium for imposed surface heat flux and temperature, TN D-7176, NASA, March (1973).
4. R. Siegel and A. Snyder, Analysis of coolant entrance boundary shape of porous region to control cooling along exit boundary, *Trans. Am. Soc. Mech. Engrs*, Series C, *J. Heat Transfer* **105,** 513–518 (1983).
5. R. Siegel and M. E. Goldstein, Analysis of heat transfer in a porous cooled wall with variable pressure and temperature along the coolant exit boundary, TN D-6621, NASA, January (1972).
6. P. M. Morse and H. Feshbach, *Methods of Theoretical Physics*, Part I, p. 689. McGraw-Hill, New York (1953).
7. R. H. Nilson and Y. G. Tsuei, Inverted Cauchy problem for the Laplace equation in engineering design, *J. Engng Math.* **8,** 329–337 (1974).
8. M. Abramowitz and I. A. Stegun, *Handbook of Mathematical Functions*, NBS Applied Mathematics Series No. 55, pp. 592–593. National Bureau of Standards, Washington, DC (1967).

FORME D'UNE REGION POREUSE POUR LE REFROIDISSEMENT LE LONG D'UNE FRONTIERE COURBE DE SORTIE

Résumé—Une insertion poreuse refroidie dans une paroi courbe est soumise à un flux thermique variable spatialement et appliqué sur un seul coté. On désire contrôler la distribution du flux de refroidissement à travers cette surface courbe de façon que la surface prenne une température uniforme fixée. La régulation de l'écoulement est obtenue en choisissant la forme de la surface à travers laquelle le réfrigérant pénètre pour obtenir la variation requise de résistance à l'écoulement dans la région. La forme appropriée de la surface est trouvée en résolvant un problème de Cauchy. Des solutions analytiques sont données en bidimensionnel pour différentes formes de la frontière chaude soumises à différentes distributions de chauffage.

DIE FORM EINES PORÖSEN BEREICHS ZUR REGELUNG DER KÜHLUNG AN EINER GEKRÜMMTEN FLÄCHE

Zusammenfassung—Der gekühlte poröse Einsatz in einer gekrümmten Wand wird an einer Seite mit einem bestimmten, örtlich variierenden Wärmestrom beaufschlagt. Das Ziel ist, die Verteilung des Kühlmittelstroms durch diese gekrümmte Fläche so zu regeln, daß die Oberfläche auf der gewünschten einheitlichen Temperatur gehalten wird. Die Regelung des Kühlmittelstroms wird dadurch erreicht, daß der Querschnitt, durch den das Kühlmittel eintritt, entsprechend geformt wird, um die erforderliche Variation des Strömungswiderstandes innerhalb des Bereichs zu erhalten. Die richtige Form der Oberfläche wird durch Lösung eines Cauchyschen Randwertproblems erhalten. Analytische Lösungen werden zweidimensional für verschiedene Formen des beheizten Randes und verschiedene Verteilungen der Heizleistung angegeben.

ВЫБОР КОНФИГУРАЦИИ ПОРИСТОЙ ОБЛАСТИ ДЛЯ УПРАВЛЕНИЯ ПРОЦЕССОМ ОХЛАЖДЕНИЯ ВДОЛЬ ИСКРИВЛЕННОЙ ГРАНИЦЫ НА ВЫХОДЕ

Аннотация—Одна из сторон охлаждаемой пористой вставки, помещенной в стенку с искривленной поверхностью, нагревается тепловым потоком заданной пространственно изменяющейся интенсивности. Необходимо выяснить возможность управления распределением потока охладителя, вытекающего через эту искривленную поверхность, с тем чтобы поверхность могла поддерживаться при заданной однородной температуре. Регулирование потоком осуществляется за счет придания определенной формы поверхности, через которую втекает охладитель, с тем чтобы можно было получить требуемое изменение гидравлического сопротивления в этой области. Необходимая форма поверхности найдена путем решения граничной задачи Коши. Даны двумерные аналитические решения для различных конфигураций нагреваемой границы, на которой имеют место различные распределения теплового потока.